Acta Mech 226, 3069–3084 (2015)
DOI 10.1007/s00707-015-1375-6

ORIGINAL PAPER

H. H. Zhu · Q. Chen · J. W. Ju · Z. G. Yan · F. Guo · Y. Q. Wang · Z. W. Jiang · S. Zhou · B. Wu

Maximum entropy-based stochastic micromechanical model for a two-phase composite considering the inter-particle interaction effect

Received: 20 January 2015 / Revised: 6 April 2015 / Published online: 9 May 2015

Abstract A maximum entropy-based stochastic micromechanical framework considering the inter-particle interaction effect is proposed to characterize the probabilistic behavior of the effective properties of two-phase composite materials. Based on our previous work, the deterministic micromechanical model of the two-phase composites is derived by introducing the strain concentration tensors considering the inter-particle interaction effect. By modeling the volume fractions and properties of constituents as stochastic, we extend the deterministic framework to stochastics, to incorporate the inherent randomness of effective properties among different specimens. A distribution-free method is employed to get the unbiased probability density function based on the maximum entropy principle. Further, the normalization procedures are utilized to make the probability density functions more stable. Numerical examples including limited experimental validations, comparisons with existing micromechanical models, commonly used probability density functions and the direct Monte Carlo simulations indicate that the proposed models provide an accurate and computationally efficient framework in characterizing the effective properties of two-phase composites.

H. H. Zhu · Q. Chen (✉) · J. W. Ju · Z. G. Yan · S. Zhou
Key Laboratory of Geotechnical and Underground Engineering of the Ministry of Education, Tongji University, 1239 Siping Road, Shanghai 200092, China
E-mail: 13585546170@163.com; chenqing19831014@163.com

H. H. Zhu · Q. Chen · J. W. Ju · Z. G. Yan · S. Zhou
State Key Laboratory for Disaster Reduction in Civil Engineering, Tongji University, 1239 Siping Road, Shanghai 200092, China

Q. Chen · Z. W. Jiang
Key Laboratory of Advanced Civil Engineering Materials of Ministry of Education, Tongji University, Shanghai 200092, China

J. W. Ju
Department of Civil and Environmental Engineering, University of California, Los Angeles, CA 90095-1593, USA

F. Guo
Department of Statistics, Virginia Tech, Blacksburg, VA 24060, USA

Q. Chen · Y. Q. Wang
Shaanxi Provincial Major Laboratory for Highway Bridge and Tunnel, Chang'an University, Xi'an, 710064 Shaanxi, China

B. Wu
State Key Laboratory of Subtropical Building Science, South China University of Technology, Guangzhou, 510640 Guangdong, China

1 Introduction

The quantification of effective linear elastic properties of composites with complex microstructures is warranted in many areas of material sciences, such as epoxy composites, ceramic matrix composites, porous and cracked media, concrete, polymer-blended soils and rocks [1].

To tackle this class of problems, many methods have been developed in the literature. Eshelby [2–4] derived the elastic field inside and outside an ellipsoidal inclusion in an infinite medium and proposed the celebrated *equivalent inclusion principle* to relate the elastic inclusions and inhomogeneities. Hashin and Shtrikman [5–7] employed variational principles to obtain the lower and upper bounds for effective properties of multiphase particulate composites. Torquato [8] presented the improved higher-order statistical bounds of two-phase linear composites. Willis [9] proposed the nonlinear variation bounds for composites. Examples for an application of the Willis method can be found in Beran and Molyneux [10], and Willis [11]. By introducing the effective medium to incorporate the influence of surrounding particles, a category of micromechanical methods was developed, such as the self-consistent method [12], the differential scheme [13], the Mori–Tanaka method [14,15] and the generalized self-consistent method [16]. The effective medium methods were utilized to estimate the effective properties of rocks [17–19] and concrete [20–24]. Yang et al. [25] employed the effective medium method to predict the effective properties of composites with multi-inclusions. Garboczi and Berryman [26] compared the results obtained by the effective medium method with those of finite element computations. Another attractive methodology attempted to directly determinate the effective properties of composites with randomly located particles by approximations or by assuming certain special configurations for particles (inhomogeneities) dispersing in matrix materials [27–30]. This micromechanical direct-interaction homogenization framework by Ju et al. [31–34] was systematically employed to predict the effective properties of fiber reinforced composites and the elastoplastic behavior of metal matrix composites. By taking the direct interparticle interactions, imperfect interfacial bonding and particle size effects into consideration, this new class of methodology was further developed by Ju et al. [35–38].

Due to the difficulties in detailing the exact predetermined microstructural composites, there is an inherent randomness of microstructures even under the same manufacturing process [39]. However, the aforementioned approaches are deterministic in nature, and the inputs for estimating effective properties are usually the volume average or ensemble average of microstructural features. The deterministic approach does not consider the stochastic behavior of composites observed in actual specimens [39]. To address this shortcoming, stochastic multi-scale analyses for heterogeneous materials had been developed in the literature [40–47]. The primary premise is that the stochastic behavior of macroscopic properties is a result of random microstructures of materials. As an important part of stochastic multi-scale analysis for random materials, some stochastic micromechanical models were presented for functionally graded materials [39,48,49]. Xu and Graham-Brady [50] presented a stochastic computational method to evaluate the global effective properties and local probabilistic behavior of random elastic media. To quantify the size effect of RVE, the generalized variational principles were adapted by Xu and Chen [51] to stochastic homogenization problems, which resulted in size-dependent energy bounds and Hashin–Shtrikman bounds. The authors proposed a stochastic micromechanical framework for multiphase composites to characterize the probabilistic behavior of effective properties of composite materials [52]. Within this framework, the deterministic micromechanical models were derived by ignoring the inter-particle interaction effect, and the probability density functions (pdfs) of the effective properties were obtained by a new simulation framework, consisting of a univariate approximation for a function with multivariate random variables, Newton interpolations and Monte Carlo simulation. Furthermore, it is difficult to get the accurate pdfs with the limited samples. The traditional approach, which is distribution-dependent, to tackle this problem is as follows. The common pdfs such as the lognormal, normal and Weibull distributions are employed to approximate the real distribution, and then, parameters of the assumed distributions are obtained via the parameter estimation method [53]. As an extension of our previous works [28,29,52], on one hand, the deterministic micromechanical models were derived by considering the inter-particle interaction effect; on the other hand, a distribution-free method is utilized to obtain the unbiased pdfs of the effective properties based on the maximum entropy principle, which is not subjected to the forms of assumed standard theoretical distribution [54–56].

An outline of this paper is as follows. Section 2 introduces the representative volume element (RVE) description for the microstructures of engineering composite materials. In Sect. 3, the solutions for the strain concentration tensors considering the inter-particle interaction effect are obtained for a spherical inhomogeneity, which form our deterministic formulas for estimating the effective moduli of two-phase composites. In Sect. 4, a stochastic micromechanical model is presented to incorporate the inherent fluctuations of the effective

properties. A distribution-free method is employed to attain the unbiased probability density function based on the maximum entropy principle. Further, the normalization procedures are utilized to make the results more stable. In Sect. 5, numerical examples including limited experimental validations, comparisons with existing micromechanical models, commonly used probability density functions and the Monte Carlo simulations indicate that the proposed new models provide both accurate and computationally efficient frameworks to characterize the effective properties of specific two-phase composites.

2 Description by a representative volume element (RVE)

The representative volume element (RVE) is based on a "mesoscopic" length scale which is much larger than the characteristic length scale of particles (inhomogeneities) but smaller than the characteristic length scale of a macroscopic specimen [28]. The RVE is developed based on the assumption that the microstructure of the heterogeneous material is known. The input for the RVE for the deterministic micromechanical framework is usually volume average or ensemble average of the descriptors of the microstructures. For example, when a group of blocks made under the same process is considered, the volume average or ensemble average of the volume fraction can be defined as below [57]:

$$\langle c(\mathbf{x})\rangle = \lim_{N\to\infty}\frac{1}{N}\sum_{\alpha=1}^{N} c(\mathbf{x},\alpha) \quad \text{and} \quad \overline{c(\alpha)} = \lim_{M\to\infty}\frac{1}{V}\sum_{i=1}^{M} c(\mathbf{x}_i,\alpha)V_i. \tag{1}$$

Here, $c(\mathbf{x},\alpha)$ is the local particle volume fraction of the sample α at $\mathbf{x}$; N is the number of the samples; $c(\mathbf{x}_i,\alpha)$ is the local volume fraction of the αth block which is divided into M subdomains of volume V_i, where $\sum_{i=1}^{M} V_i = V$, with V being the total volume of the block; $\mathbf{x}_i$ signifies the coordinate of a representative point for subdomain V_i. Further, $\overline{c(\alpha)}$ and $\langle c(\mathbf{x})\rangle$ are the volume average and ensemble average of the volume fraction, respectively. For statistically homogeneous materials, the volume average and the ensemble average are equal to each other.

In reality, the microstructures of engineering materials are complex and often random in nature. Stochastic descriptions are introduced to reflect the influence of the inherent random microstructures on the macroscopic properties [39,48,49,52]. By changing the input into random fields or random variables from the volume average or ensemble average of the descriptors for microstructures, the probabilistic behavior of effective properties of the composites can be characterized by the stochastic micromechanical framework [39,48,49,52].

3 Deterministic micromechanical framework for a two-phase composite considering the inter-particle interaction

The deterministic micromechanical model in this section is derived based on the RVE description for the microstructure [28–38]. In this model, all particles are assumed to be spherical, non-intersecting (impenetrable) and embedded firmly into a homogeneous matrix material; i.e., perfect interfacial bonding is assumed. Further, the composite and all its constituents are supposed to be elastic and isotropic.

3.1 Definition for effective properties and strain concentration tensors

When a two-phase composite is considered, the "strain concentration tensor" $\mathbf{B}$ can be defined for the inhomogeneity by [57]

$$\bar{\boldsymbol{\varepsilon}}_1 = \mathbf{B} : \bar{\boldsymbol{\varepsilon}} \tag{2}$$

where $\bar{\boldsymbol{\varepsilon}}_1$ is the volume average strain on the inhomogeneity and $\bar{\boldsymbol{\varepsilon}}$ is the volume average strain of the composite.

The effective stiffness tensor of the two-phase composite can be derived by [28–38,57]

$$\mathbf{C}_* = [\mathbf{C}_0 + \phi_1 (\mathbf{C}_1 - \mathbf{C}_0) : \mathbf{B}] \tag{3}$$

where $\mathbf{C}_*$ is the effective elastic stiffness tensor of the composite; $\mathbf{C}_0$ and $\mathbf{C}_1$ are the elastic stiffness tensor of the matrix phase and the inhomogeneity, respectively; ϕ_1 is the volume fraction of the inhomogeneity.

The strain concentration tensor is the only unknown in typical engineering applications. In the next section, the strain concentration tensor will be derived considering the inter-particle interaction effect.

3.2 Solution for the strain concentration tensors considering the inter-particle interaction effect

According to Eshelby's equivalence principle [2–4], the perturbed strain field $\boldsymbol{\varepsilon}'(\mathbf{x})$ induced by an inhomogeneity can be related to specified eigenstrains $\boldsymbol{\varepsilon}^*(\mathbf{x})$ by replacing the inhomogeneity with the matrix material (or vice versa). It is noted that $\boldsymbol{\varepsilon}^*(\mathbf{x})$ is *nonzero* in the particle domain and *zero* in the matrix domain. For the domain of the particles with elastic stiffness tensor $\mathbf{C}_1$, we have

$$\mathbf{C}_1 : \left[\boldsymbol{\varepsilon}^0 + \boldsymbol{\varepsilon}'(\mathbf{x})\right] = \mathbf{C}_0 : \left[\boldsymbol{\varepsilon}^0 + \boldsymbol{\varepsilon}'(\mathbf{x}) - \boldsymbol{\varepsilon}^*(\mathbf{x})\right] \tag{4}$$

where $\boldsymbol{\varepsilon}^0$ is the uniform strain field induced by far-field loads for a homogeneous matrix material only.

Let us define $\bar{\boldsymbol{\varepsilon}}^{*0}$as the volume average of the "noninteracting" solution for the eigenstrains and $\bar{\boldsymbol{\varepsilon}}_1^{*0}$ as its value in the particle domain. According to the work of Ju and Chen [28], Eq. (4) can be rephrased as follows:

$$-\mathbf{A}_1 : \bar{\boldsymbol{\varepsilon}}_1^{*0} = \boldsymbol{\varepsilon}^0 + \mathbf{S} : \bar{\boldsymbol{\varepsilon}}_1^{*0} \tag{5}$$

with

$$\mathbf{A}_1 \equiv (\mathbf{C}_1 - \mathbf{C}_0)^{-1} : \mathbf{C}_0, \tag{6}$$

$$S_{ijkl} = \frac{1}{15(1-\nu_0)}\left[(5\nu_0 - 1)\delta_{ij}\delta_{kl} + (4 - 5\nu_0)(\delta_{ik}\delta_{jl} + \delta_{il}\delta_{jk})\right] \tag{7}$$

We refer to reference [58] for details.

Further, let $\boldsymbol{\varepsilon}^{*p}$ denote the solution for the eigenstrains considering the inter-particle interaction effect. According to the work of Ju and Chen [29], the volume average of this eigenstrains $\bar{\boldsymbol{\varepsilon}}^{*p}$ can be given by

$$\bar{\boldsymbol{\varepsilon}}^{*p} = \boldsymbol{\Gamma} : \bar{\boldsymbol{\varepsilon}}^{*0} \tag{8}$$

with

$$\Gamma_{ijkl} = \gamma_1 \delta_{ij}\delta_{kl} + \gamma_2\left(\delta_{ik}\delta_{jl} + \delta_{il}\delta_{jk}\right), \tag{9}$$

$$\gamma_1 = \frac{5\phi}{96\beta^2}\left\{12\nu_0(13 - 14\nu_0) - \frac{96\alpha}{3\alpha + 2\beta}(1 - 2\nu_0)(1 + \nu_0)\right\}, \tag{10}$$

$$\gamma_2 = \frac{1}{2} + \frac{5\phi}{96\beta^2}\left\{6(25 - 34\nu_0 + 22\nu_0^2) - \frac{36\alpha}{3\alpha + 2\beta}(1 - 2\nu_0)(1 + \nu_0)\right\}, \tag{11}$$

$$\alpha = 2(5\nu_0 - 1) + 10(1 - \nu_0)\left(\frac{K_0}{K_1 - K_0} - \frac{\mu_0}{\mu_1 - \mu_0}\right), \tag{12}$$

$$\beta = 2(4 - 5\nu_0) + 15(1 - \nu_0)\frac{\mu_0}{\mu_1 - \mu_0}. \tag{13}$$

The "strain concentration tensor" $\mathbf{B}$ for the spherical inhomogeneity of the two-phase composite can be obtained by [29]

$$\mathbf{B} = \boldsymbol{\Gamma}\,\mathbf{A}_1(\mathbf{A}_1 + \mathbf{S} - \phi_1\mathbf{S}\,\boldsymbol{\Gamma})^{-1}. \tag{14}$$

The effective stiffness tensor can be characterized as

$$\mathbf{C}^* = \mathbf{C}_0\left\{\mathbf{I} - \phi\boldsymbol{\Gamma}(-\mathbf{A}_1 - \mathbf{S} + \phi_1\mathbf{S}\boldsymbol{\Gamma})^{-1}\right\}. \tag{15}$$

We follow Ju et al. [28–38] to conduct analytical examples using the proposed micromechanical framework. K^*, μ^* and E^* represent the effective bulk modulus, shear modulus and Young's modulus of the two-phase composite, respectively. When the inter-particle interaction effect is considered, the effective bulk modulus and shear modulus of the two-phase composite are as follows:

$$K^* = K_0\left\{1 + \frac{30(1 - \nu_0)\phi_1(3\gamma_1 + 2\gamma_2)}{3\alpha + 2\beta - 10(1 + \nu_0)\phi_1(3\gamma_1 + 2\gamma_2)}\right\}, \tag{16}$$

$$\mu^* = \mu_0\left\{1 + \frac{30(1 - \nu_0)\phi_1\gamma_2}{\beta - 4(4 - 5\nu_0)\phi_1\gamma_2}\right\} \tag{17}$$

where K_0, μ_0, ν_0 are the bulk modulus, shear modulus and Poisson's ratio of the matrix, respectively, and K_1, μ_1, ν_1 are those of the inhomogeneity, respectively. Moreover, ϕ_1 is the volume fraction of the inhomogeneity. Therefore, the effective Young's modulus for the two-phase composite can be simply computed from the following well-known expression:

$$E^* = \frac{9K^*\mu^*}{3K^* + \mu^*}. \tag{18}$$

4 Maximum entropy-based stochastic micromechanical framework for two-phase composites

Based on the deterministic micromechanical framework in the above section, the effective properties of the two-phase composites can be estimated with the volume average or ensemble average of the descriptors for microstructures. However, in real engineering problems, there is an inherent randomness of the specimen even under the same manufacturing process. To consider these fluctuations, the input of the micromechanical predicting model should be random [39,57]. Therefore, in this section, the volume fraction and the material properties of the constituents in the two-phase composites are described by appropriate random variables. Accordingly, our proposed micromechanical model is readily extended to a stochastic framework.

4.1 Stochastic description for microstructures of two-phase composites

Let $(\mathbf{\Omega}, \boldsymbol{\xi}, P)$ be a probability space, where $\mathbf{\Omega}$ is the sample space, $\boldsymbol{\xi}$ is the σ-algebra of subsets of $\mathbf{\Omega}$, and P is the probability measure, and $\mathbf{R}^N$ be an N-dimensional real vector space. Further, we define ϕ_0, E_0, ν_0 as the volume fraction, the elastic modulus and Poisson's ratio of the matrix phase, respectively. Then $\phi_0 = 1 - \phi_1$, which means that the volume fractions of the components are not independent. Therefore, the random vector $\{E_0, E_1, \nu_0, \nu_1\}^T \in \mathbf{R}^4$ describes stochastic elastic properties of the composite. The probability density function of constituent material properties is either assumed or derived from available material characterization data. Hence, an input random vector $\{E_0, E_1, \nu_0, \nu_1, \phi_1\}^T \in \mathbf{R}^5$ characterizes uncertainties from all sources in a two-phase composite based on our proposed micromechanical model. The characterization of effective properties of a two-phase composite containing spherical inhomogeneity becomes a problem of characterization of a random function with multivariate random variables. In the next section, the maximum entropy principle is employed to get the unbiased probability density function of the effective properties. Further, the normalization procedures of the random function with multivariate random variables are utilized to make the results more stable.

4.2 Maximum entropy-based probability density function for effective properties

4.2.1 Maximum entropy principle

In information theory, entropy is a measure of the uncertainty associated with a random variable. In mathematical terms, let us consider a continuous random variable x with the probability density function $f(x)$ in the domain of variable definition R. The entropy H is defined as

$$H = -\int_R f(x)\ln[f(x)]\mathrm{d}x. \tag{19}$$

The maximum entropy principle was developed by Jaynes [54] on the basis of the concept of statistical entropy, as a rational approach for choosing a consistent probability distribution among all possible distributions. The principle states that the minimally prejudiced probability distribution is the one that maximizes the entropy subject to constraints, for example, the moments of a random variable.

Assume that m_i is the ith origin moment of random variable x. Then

$$\int_R^{f(x)} \mathrm{d}x - 1 = 0, \tag{20}$$

$$\int_R x^i f(x)\mathrm{d}x - m_i = 0. \tag{21}$$

Equations (20) and (21) represent the normalization condition and the moment conditions, respectively. The Euler–Lagrange equation can be applied to solve the function maximum problem, and the solution can be expressed as follows [55]:

$$f(x) = \exp\left[a_0 + \sum_{i=1}^{N} a_i x^i\right] \tag{22}$$

where a_i, $i = 0, 1, 2, \ldots, n$ are the Lagrangian multipliers. According to the work of [55,59], these parameters can be obtained by solving the following equations:

$$\begin{bmatrix} 1 & m_1 & \cdots & m_{n-1} \\ m_1 & m_2 & \cdots & m_n \\ \vdots & \vdots & \ddots & \vdots \\ m_{n-1} & m_n & \cdots & m_{2n-2} \end{bmatrix} \begin{bmatrix} a_1 \\ 2a_2 \\ \vdots \\ na_n \end{bmatrix} = \begin{bmatrix} 0 \\ -1 \\ -2m_1 \\ \vdots \\ -(n-1)m_{n-2} \end{bmatrix}, \tag{23}$$

$$a_0 = \ln\left(\frac{1}{\int_{-\infty}^{+\infty} \mathrm{e}^{a_1 x + a_2 x^2 + \cdots a_n x^n} \mathrm{d}x}\right). \tag{24}$$

It is noted that the moment matrix in Eq. (23) usually becomes singular, when the number of parameters becomes large. It will lead to distorted results for unknown parameters [59]. In such situation, the nonlinear optimization program is usually utilized due to the mathematical difficulties in solving analytic relations between the moments and distribution parameters [55]. Fortunately, good predicting results can be reached in most cases when the fourth- or sixth-order moments are considered according to [59]. Therefore, instead of adopting the nonlinear optimization program, normalization procedures are employed to make the predicting results more stable.

4.2.2 Normalization procedures

Let us define μ_x and σ_x as the mean and standard deviation of x, respectively. The normalized variable $\bar{x}$ is obtained as follows:

$$\bar{x} = \frac{x - \mu_x}{\sigma_x}. \tag{25}$$

$\bar{f}(\bar{x})$ is taken as the pdf of the normalized variable $\bar{x}$, which can be reached by solving the following equations according to the maximum entropy principle:

$$\begin{bmatrix} 1 & 0 & \cdots & \bar{m}_{n-1} \\ 0 & 1 & \cdots & \bar{m}_n \\ \vdots & \vdots & \ddots & \vdots \\ \bar{m}_{n-1} & \bar{m}_n & \cdots & \bar{m}_{2(n-1)} \end{bmatrix} \begin{Bmatrix} \bar{a}_1 \\ 2\bar{a}_2 \\ \vdots \\ n\bar{a}_n \end{Bmatrix} = \begin{Bmatrix} 0 \\ -1 \\ \vdots \\ -(n-1)\bar{m}_{n-2} \end{Bmatrix}, \tag{26}$$

$$\bar{a}_0 = \ln\left(\frac{1}{\int_{-\infty}^{+\infty} \mathrm{e}^{\bar{a}_1 x + \bar{a}_2 x^2 + \cdots \bar{a}_n x^n} \mathrm{d}x}\right) \tag{27}$$

where $\bar{a}_i$, $i = 0, 1, 2, \ldots, n$ are the Lagrangian multipliers for the normalized variable $\bar{x}$; $\bar{m}_i$, $i = 1, 2, \ldots, n$ are the different order moments for $\bar{x}$. With the pdf $\bar{f}(\bar{x})$ of normalized variable $\bar{x}$, the pdf $f(x)$ of variable x can be obtained as follows:

$$f(x) = \frac{1}{\sigma_x} \bar{f}\left(\frac{x - \mu_x}{\sigma_x}\right). \tag{28}$$

4.2.3 The application of the maximum entropy principle in the stochastic micromechanical models

The unbiased pdfs of the effective properties can be calculated with the maximum entropy principle. By the stochastic descriptions of the microstructures, the effective properties of the two-phase composite turn to a random function with multivariate random variables based on our proposed deterministic micromechanical model. Hence, the effective moduli, such as K^*, μ^* or E^*, can be regarded as random variables, which can be represented by x.

With Eqs. (26)–(27), the maximum entropy-based pdfs $\bar{f}(\bar{x})$ for the normalized random variable $\bar{x}$ can be calculated with its different order moments. The corresponding pdfs $f(x)$ for the random variable x can be obtained by Eq. (28) with the means, standard deviations of x. The Monte Carlo simulation and statistical analysis are adopted to obtain statistical characteristics of $\bar{x}$ and x, which represent the (normalized) effective properties in our stochastic micromechanical framework.

According to our proposed determined micromechanical model, the effective properties corresponding to a random input of microstructures can be calculated by Monte Carlo simulation on Eqs. (16)–(18). The mean and standard deviation of the effective bulk modulus, shear modulus and Young's modulus can be obtained by the following statistical analysis:

$$\text{mean}\left(K^*\right) = \frac{1}{M}\sum_{m=1}^{M}\left(K_m^*\right), \quad \text{sd}\left(K^*\right) = \sqrt{\left(\frac{1}{M}\sum_{m=1}^{M}\left(K_m^* - \text{mean}\left(K^*\right)\right)^2\right)^{1/2}}, \tag{29}$$

$$\text{mean}\left(\mu^*\right) = \frac{1}{M}\sum_{m=1}^{M}\left(\mu_m^*\right), \quad \text{sd}\left(\mu^*\right) = \sqrt{\left(\frac{1}{M}\sum_{m=1}^{M}\left(\mu_m^* - \text{mean}\left(\mu^*\right)\right)^2\right)^{1/2}}, \tag{30}$$

$$\text{mean}\left(E^*\right) = \frac{1}{M}\sum_{m=1}^{M}\left(E_m^*\right), \quad \text{sd}\left(E^*\right) = \sqrt{\left(\frac{1}{M}\sum_{m=1}^{M}\left(E_m^* - \text{mean}\left(E^*\right)\right)^2\right)^{1/2}} \tag{31}$$

where M is the sample size; mean () and sd () denote the mean and standard deviation, respectively; K_m^*, μ_m^*, E_m^* are the *mth* sample of the effective bulk modulus, shear modulus, and Young's modulus. With the mean and standard deviation obtained above, the ith moment of the effective properties after the normalization procedures can be reached using the following formulas. Specifically, we have

$$\bar{m}_i^{K^*} = \frac{1}{M}\sum_{m=1}^{M}\left[\frac{K_m^* - \text{mean}\left(K^*\right)}{\text{sd}\left(K^*\right)}\right]^i, \tag{32}$$

$$\bar{m}_i^{\mu^*} = \frac{1}{M}\sum_{m=1}^{M}\left[\frac{\mu_m^* - \text{mean}\left(\mu^*\right)}{\text{sd}\left(\mu^*\right)}\right]^i, \tag{33}$$

$$\bar{m}_i^{E^*} = \frac{1}{M}\sum_{m=1}^{M}\left[\frac{E_m^* - \text{mean}\left(E^*\right)}{\text{sd}\left(E^*\right)}\right]^i \tag{34}$$

where $\bar{m}_i^{K^*}$, $\bar{m}_i^{\mu^*}$ and $\bar{m}_i^{E^*}$ stand for the ith moments of the normalized effective bulk modulus, shear modulus and Young's modulus, respectively.

By replacing $\bar{m}_i$ in Eq. (26) with $\bar{m}_i^{K^*}$, $\bar{m}_i^{\mu^*}$, $\bar{m}_i^{E^*}$ obtained by Eqs. (32)–(34), the coefficients for the pdfs of the normalized effective properties can be obtained, with which the pdfs of the non-normalized properties can be calculated with Eqs. (28)–(31).

5 Numerical simulations and verifications

The proposed stochastic micromechanical framework is made up of the deterministic one that we summarized in this paper (following [28–38]), the stochastic description of the microstructures and the maximum entropy-based probability density function. The verifications can be mainly classified into three categories.

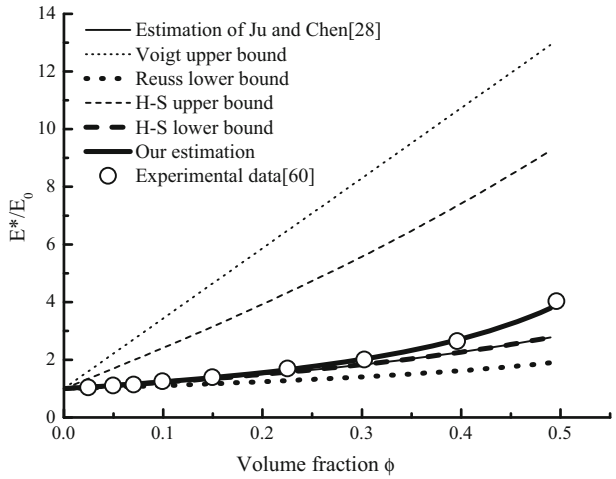

Fig. 1 Comparison among the results obtained with different micromechanical models and those obtained experimentally [60] for the effective Young's modulus

As to the deterministic micromechanical framework, the estimations of our proposed model are compared with the existing micromechanical models and available experimental data. The commonly used probability distributions, including the normal distribution, lognormal distribution and Weibull distribution, are utilized to prove the effectiveness of the maximum entropy-based probability density function. To verify the stochastic micromechanical model, our predictions are compared with the existing experimental data and the Monte Carlo simulation.

5.1 Verifications for the deterministic micromechanical models

Apart from the comparison with the Voigt upper bound, Reuss lower bound, Hashin–Shtrikman (H–S) bounds and the non-interaction solutions [28,52], the experiments conducted by Smith [60] and Walsh et al. [61] are employed to verify our deterministic micromechanical models.

Based on Eqs. (16)–(18), the effective Young's modulus of the composite can be obtained considering the inter-particle interaction. As exhibited in Fig. 1, the predictions obtained from the micromechanical model for the Young's modulus correspond well with those obtained experimentally by Smith [60]. Meanwhile, the predicted E^* lie between the upper and lower bounds reasonably. Compared with the non-interaction solutions [28,52], which coincide with Mori–Tanaka results and the H–S lower bound here [62,63], the results considering the inter-particle interaction meet better with the experimental data when the volume fraction of the particles increases.

Figure 2 shows comparisons of shear moduli between the experimental data by Smith [60] and estimations obtained by different models. Similarly, it can be found that the effective shear modulus considering the inter-particle interaction corresponds better with those obtained experimentally by Smith [60] than those non-interaction solutions [28,52], with the increase in the volume fraction of the particles. At the same time, the predicted results lie between all upper and lower bounds reasonably, including the two bounds obtained by Xu and Chen [51] for infinitely large RVE.

As to the effective bulk modulus, similar conclusions can be reached. As displayed in Fig. 3, the effective bulk modulus considering the inter-particle interaction corresponds better to the experimental data obtained by Walsh et al. [61] when the volume fraction of the particles becomes higher. Similarly, our predictions are always lower than the upper bounds (Voigt upper bound and H–S upper bound) and higher than lower bounds (Reuss lower bound and H–S lower bound).

5.2 Verifications for the effectiveness of the maximum entropy-based probability density function

Since it is hard to get the accurate pdfs of the macroscopic properties of materials, common distribution types, such as the normal distribution, lognormal distribution and Weibull distribution, are employed to approximate

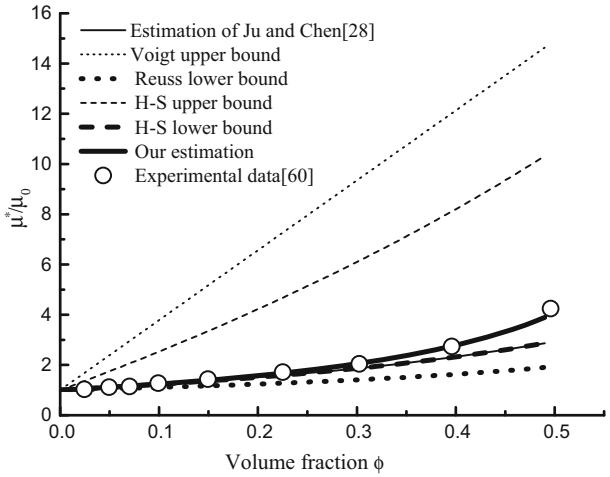

Fig. 2 Comparison among the results obtained with different micromechanical models and those obtained experimentally [60] for the effective shear modulus

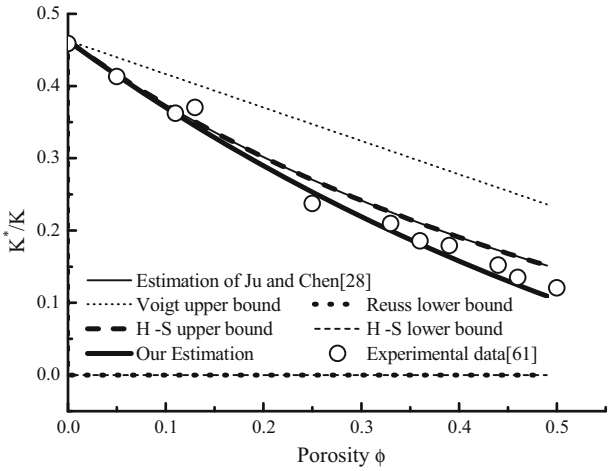

Fig. 3 Comparison among the results obtained with different micromechanical models and those obtained experimentally [61] for the effective bulk modulus

the real distribution with certain prior assumptions [52,53]. Our proposed distribution-free method is capable of representing all these distributions without any premise. In this section, these commonly used probability distributions are utilized to test the effectiveness of our maximum entropy-based pdfs.

Table 1 shows all the distribution types we employed. Figure 4a–e represents comparisons between our maximum entropy- based probability density function and those commonly used probability distributions. In these cases, to get the moments of the random variables, 10^3 sample points are used. It can be found that our maximum entropy-based probability density function can approximate those distributions well when fourth-order moments are considered. Further, the approximations become better when the sixth-order moments are utilized.

The sample size will influence the accuracy of our maximum entropy-based pdfs. To address this issue, moments obtained by different sample sizes are used to get the pdfs, which are compared with the theoretical solution. Figure 5 shows the comparisons between the pdfs obtained by different sample sizes and the theoretical value for the normal distribution. It can be seen that the approximations become better with the increase in the number of sample points. When 10^3 sample points are adopted, the maximum entropy-based pdf corresponds well to the theoretical solution. As to the lognormal distribution, similar conclusions can be reached from Fig. 6.

The normalization procedures can make the maximum entropy-based pdfs more stable when higher-order moments are utilized. Table 2 shows the coefficients obtained using the maximum entropy principle with and

Table 1 Common distribution types employed in this paper

Number	Distribution type	Probability density function	Parameter values
1	Normal	$f(x) = \frac{1}{\sigma\sqrt{2\pi}} \mathrm{e}^{-\frac{(x-\mu)^2}{2\sigma^2}}$	$\mu = 100,\ \sigma = 15$
2	Lognormal	$f(x) = \frac{1}{x\sigma\sqrt{2\pi}} \mathrm{e}^{-\frac{(\ln x-\mu)^2}{2\sigma^2}}$	$\mu = 10,\ \sigma = 1$
3	Weibull	$f(x) = \begin{cases} \frac{k}{\lambda}\left(\frac{x}{\lambda}\right)^{k-1} \mathrm{e}^{-(x/\lambda)^k} & x \geq 0 \\ 0 & x < 0 \end{cases}$	$\lambda = 3,\ k = 6$
4	Gamma	$f(x) = \begin{cases} \frac{1}{b^a \Gamma(a)} x^{a-1} x^{-\frac{x}{b}} & x \geq 0 \\ 0 & x < 0 \end{cases}$	$a = 15,\ b = 3$
5	Extreme value	$f(x) = \frac{1}{\sigma} \mathrm{e}^{\left(\frac{x-\mu}{\sigma}\right)} \mathrm{e}^{-\mathrm{e}^{\left(\frac{x-\mu}{\sigma}\right)}}$	$\mu = -2,\ \sigma = 2$

without the normalization procedure. It can be found that all the coefficients are still stable when the sixth-order moments are used with the normalization procedure. However, without the normalization procedures, the coefficient a_0 will not exist at such situation. Similar conclusions can be reached when the lognormal distribution is considered, which is exhibited by Table 3.

5.3 Verifications for the stochastic micromechanical framework

The stochastic micromechanical models can be applied to evaluate the effective properties of functionally graded materials (FGM) [39,49,52]. To verify our stochastic model, the high–low experimental data of Parameswaran and Shukla [64] are employed. The properties of constituent materials are independent lognormal random variables whose means and coefficients of variation are defined in [49]. Since the range of the volume fraction is between 0 and 1, the distribution type is considered to be a beta distribution [49]. Hence, the probability density function $f(\phi)$ takes the form:

$$f(\phi) = \begin{cases} \frac{1}{B(\alpha,\beta)} \phi^{\alpha-1} (1-\phi)^{\beta-1}, & 0 \leq \phi \leq 1 \\ 0, \quad \text{otherwise} \end{cases} \tag{35}$$

with

$$B(\alpha, \beta) = \frac{\Gamma(\alpha)\,\Gamma(\beta)}{\Gamma(\alpha+\beta)}, \tag{36}$$

$$\Gamma(\tau) = \int_0^\infty \exp(-\eta)\eta^{\tau-1} d\eta\ , \ \text{with}\ \tau = \alpha\ \text{or}\ \beta \quad \text{for}\ \Gamma(\alpha)\ \text{or}\ \Gamma(\beta) \tag{37}$$

where α and β are distribution parameters. Moreover, $B(\alpha, \beta)$ is the beta function, and $\Gamma(\tau)$ is the gamma function. According to the work of [49], the means mean(ϕ) and the standard deviations SD(ϕ) for the volume fraction of particles at different places can be expressed as follows:

$$\text{mean}(\phi) = 0.109x + 4.25x^2 - 9.762x^3 + 8.629x^4 - 2.748x^5, \tag{38}$$

$$\text{SD}(\phi) = 0.178x - 0.309x^2 + 0.155x^3 \tag{39}$$

where $x = X/T$ is the relative position along the direction of the length. Here, $T = 25\,\text{cm}$ is the total length, and X is the length from the end point, where the volume fraction of the particle is almost 0, to the point we are interested in. Further, the distribution parameters of beta distribution for different positions can be determined based on the following relationships:

$$\begin{cases} \text{mean}\,(\phi) = \frac{\alpha}{\alpha+\beta} \\ \text{SD}\,(\phi) = \sqrt{\frac{\alpha\beta}{(\alpha+\beta)^2(\alpha+\beta+1)}} \end{cases}. \tag{40}$$

Figure 7 shows the means and standard deviations of the effective Young's modulus predicted by our proposed stochastic micromechanical framework. The high–low experimental data of Parameswaran and Shukla [64],

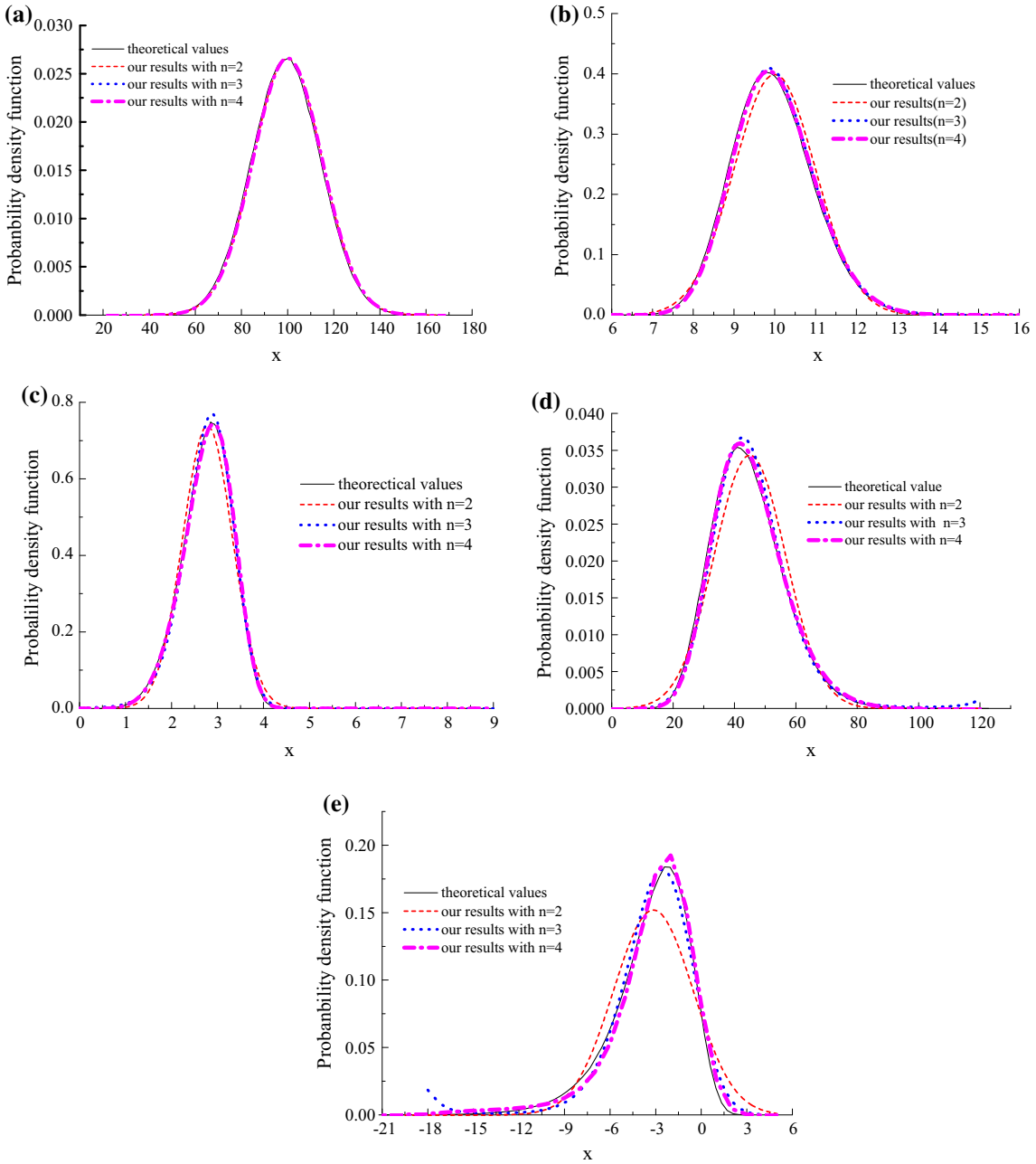

Fig. 4 Comparisons between our maximum entropy-based probability density function with different order moments and those commonly used probability distributions, where $n = 2$, $n = 3$, $n = 4$ means that second-, fourth-, sixth-order moments are used to predict the pdf. **a** The normal distribution. **b** The lognormal distribution. **c** The Weibull distribution. **d** The Gamma distribution. **e** The extreme value distribution

displayed in Fig. 7, indicate good agreement between the experimental and the predicted results. Similarly, as Fig. 8 shows, the means and standard deviations of the effective shear modulus can be obtained by our proposed stochastic micromechanical framework.

With the moments of the effective properties obtained by Monte Carlo simulation, the probability density functions of effective FGM properties can be obtained by the maximum entropy principle. Figure 9 exhibits the probability density function of the Young's modulus calculated by direct Monte carlo method and our proposed simulation framework at the position $x = X/t = 0.5$. It can be observed that the estimations of our presented framework are quite accurate compared with the direct Monte carlo simulation when the fourth-order

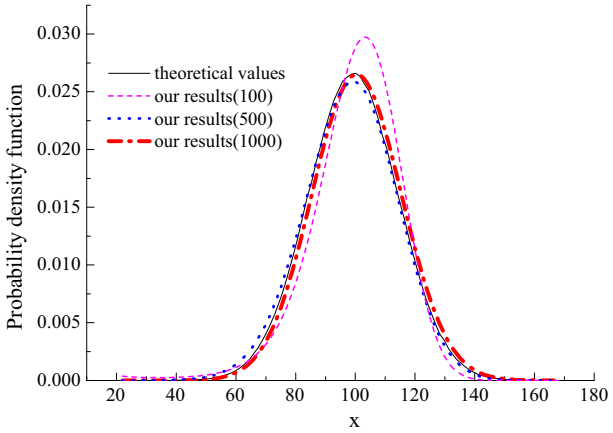

Fig. 5 Comparison between the maximum entropy-based pdfs with different sample size and the theoretical values for the normal distribution

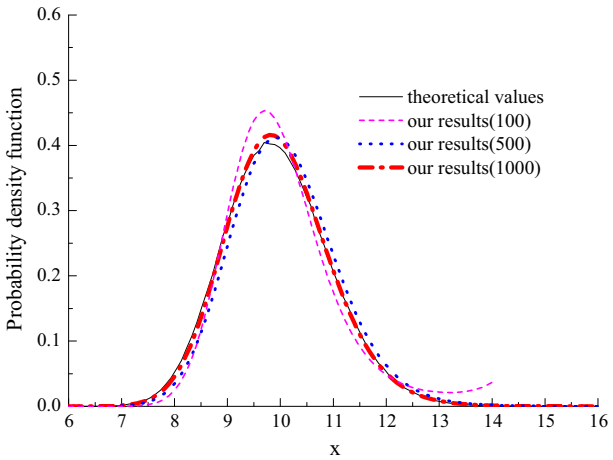

Fig. 6 Comparison between the maximum entropy-based pdfs with different sample size and the theoretical values for the lognormal distribution

Table 2 Comparison between solutions for the coefficients of the maximum entropy-based pdf for the normal distribution with and without normalization procedures

Coefficients of the pdf	$n = 2$		$n = 3$		$n = 4$	
	Non-normalized	Normalized	Non-normalized	Normalized	Non-normalized	Normalized
a_1	4.44E−01	−4.68E−13	4.42E−01	−1.38E−03	4.22E+02	−8.33E−04
a_2	−2.22E−03	−5.00E-01	−2.19E−03	−5.00E−01	6.58E+00	−5.00E−01
a_3			−9.75E−08	4.61E−04	−4.46E−02	2.78E−04
a_4					1.11E−04	5.52E−05
$e^{a_0} = c$	6.13E−12	3.99E−01	6.38E−12	3.99E−01	Inexistence	3.99E−01

Table 3 Comparison between solutions for the coefficients of the maximum entropy-based pdf for the lognormal distribution with and without normalization procedures

Coefficients of the pdf	$n = 2$		$n = 3$		$n = 4$	
	Non-normalized	Normalized	Non-normalized	Normalized	Non-normalized	Normalized
a_1	9.98E+00	4.17E−13	2.48E+01	−1.47E−01	−4.99E+04	−1.56E−01
a_2	−4.99E−01	−5.00E−01	−1.97E+00	−5.22E−01	7.39E+03	−4.97E−01
a_3			4.83E−02	4.89E−02	−4.81E+02	5.36E−02
a_4					1.16E+01	4.30E−03
$e^{a_0} = c$	8.24E−23	3.99E−01	4.02E−44	4.05E−01	Inexistence	4.00E−01

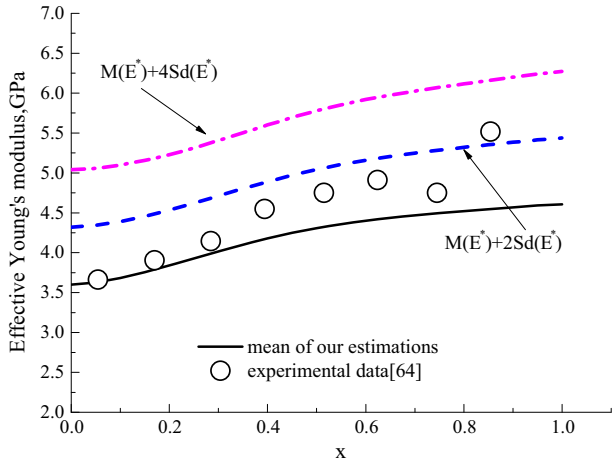

Fig. 7 Means and standard deviations of effective Young's modulus of cenosphere–polyester composite [64], with M(E*)+2Sd(E*) or 4Sd(E*) denoting means plus two times or four times of standard deviations of the Young's modulus obtained by our method

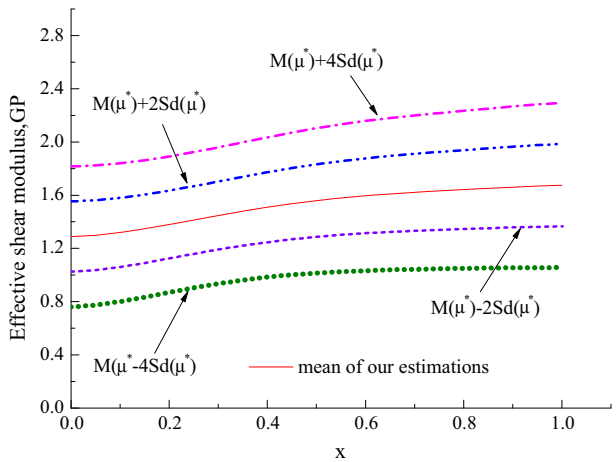

Fig. 8 Means and standard deviations of effective shear modulus of cenosphere–polyester composite [64], with M(μ^*) +/− 2Sd(μ^*) or (4Sdμ^*) denoting means plus/minus two times or four times of standard deviations of the shear modulus obtained by our method

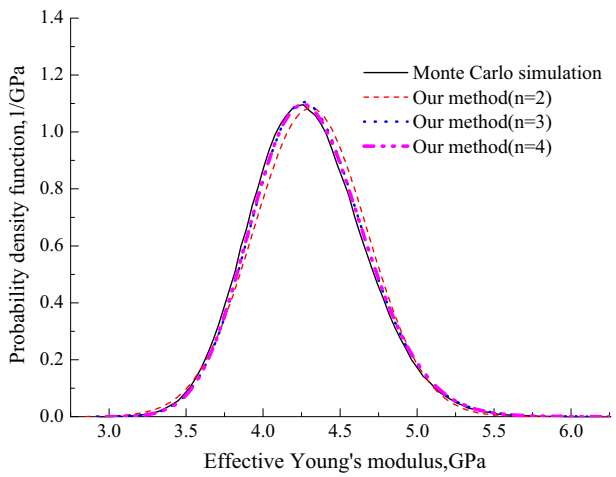

Fig. 9 Probability density functions of effective Young's modulus of cenosphere–polyester composite [64] at position $x = 0.5$, with $n = 2, n = 3, n = 4$ denoting results obtained by our method with the second-, fourth-, sixth-order moments, respectively

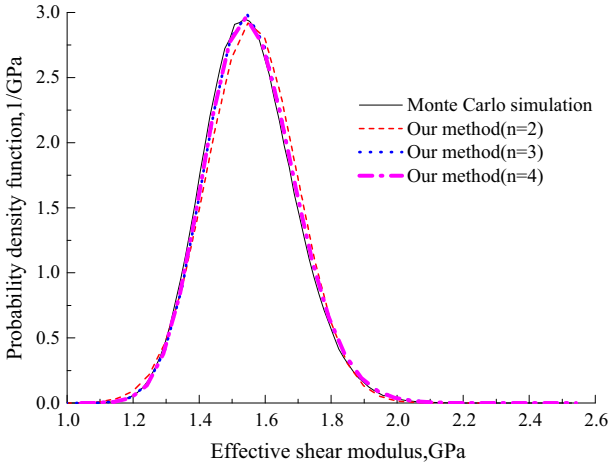

Fig. 10 Probability density functions of effective Young's modulus of cenosphere–polyester composite [64] at position $x = 0.5$, with $n = 2, n = 3, n = 4$ denoting results obtained by our method with the second-, fourth-, sixth-order moments, respectively

moments ($n = 3$) or the sixth-order moments ($n = 4$) are considered. No meaningful difference between the results of $n = 3$ and $n = 4$ is observed in this particular example. When we only consider the second-order moments ($n = 2$), the predicted pdf is still acceptable compared with the direct Monte carlo simulation. It is noted that the iterative times in solving the micromechanical equations by direct Monte carlo method is 10^6. However, the iterative times in our numerical computing can be dramatically reduced to 10^3 when our proposed simulation framework is used. Similar conclusions can be reached from the probability density function of the shear modulus, which are exhibited in Fig. 10.

6 Conclusions

Emanating from our previous work [28–38], a stochastic micromechanical framework, consisting of the proposed deterministic micromechanical model, stochastic description for the microstructures and maximum entropy-based probability density function for the random function, is presented to characterize the probabilistic behavior of the effective elastic properties of two-phase composites considering the inter-particle interactions. The normalization procedure for the random function is introduced to make the maximum entropy-based probability density more stable. To verify our proposed stochastic micromechanical framework, the predicting results are compared with the existing micromechanical models, available experimental data, commonly used probability distributions and the direct Monte Carlo simulation. Some significant conclusions can be reached as follows:

(i) The comparisons among our estimations, the results obtained by the existing micromechanical models and available experimental data show that the proposed deterministic micromechanical model can predict the effective properties of a two-phase composite well, especially when the volume fraction of the inclusion is not dilute.

(ii) The comparisons among our proposed maximum entropy-based pdfs, the commonly used pdfs and the maximum entropy-based pdfs without normalization show that the proposed maximum entropy-based pdfs can approximate the commonly used pdfs well when the fourth- or sixth-order moments are considered. The results become more stable after the normalization of the random variables. Further, the number of the sample points will influence the accuracy of our proposed maximum entropy-based pdfs. Good approximations can be obtained when this number reaches 10^3 according to our simulations.

(iii) The comparisons among our estimations, the results obtained by the Monte Carlo simulation and available experimental data illustrate that the proposed stochastic micromechanical model can predict the probabilistic behavior of elastic two-phase composites, including the means, standard deviations and probability density function. Further, our proposed new simulation framework can dramatically reduce the iterative times in solving micromechanical equations with good accuracy.

Acknowledgments This work is supported by the National Key Basic Research and Development Program (973 Program, No. 2011CB013800). This work is also supported by Shanghai Pujiang Program (14PJD034), 1000 Talents Plan Short-Term Program by the Organization Department of the Central Committee of the CPC and Research Program of State Key Laboratory for Disaster Reduction in Civil Engineering.

References

1. Torquato, S.: Random Heterogeneous Materials: Microstructure and Macroscopic Properties. Springer, Berlin (2001)
2. Eshelby, J.D.: The determination of the elastic field of an ellipsoidal inclusion, and related problems. Proc. R. Soc. Lond. Ser. A Math. Phys. Sci. **241**, 376–396 (1957)
3. Eshelby, J.D.: The elastic field outside an ellipsoidal inclusion. Proc. R. Soc. Lond. Ser. A Math. Phys. Sci. **252**, 561–569 (1959)
4. Eshelby, J.D.: Elastic inclusions and inhomogeneities. Prog. Solid Mech. **2**, 89–140 (1961)
5. Hashin, Z., Shtrikman, S.: On some variational principles in anisotropic and nonhomogeneous elasticity. J. Mech. Phys. Solids **10**, 335–342 (1962)
6. Hashin, Z., Shtrikman, S.: A variational approach to the theory of the elastic behaviour of polycrystals. J. Mech. Phys. Solids **10**, 343–352 (1962)
7. Hashin, Z., Shtrikman, S.: A variational approach to the theory of the elastic behaviour of multiphase materials. J. Mech. Phys. Solids **11**, 127–140 (1963)
8. Torquato, S.: Random heterogeneous media: microstructure and improved bounds on effective properties. Appl. Mech. Rev. **44**, 37–76 (1991)
9. Willis, J.: On methods for bounding the overall properties of nonlinear composites. J. Mech. Phys. Solids **39**, 73–86 (1991)
10. Beran, M., Molyneux, J.: Use of classical variational principles to determine bounds for the effective bulk modulus in heterogeneous media. Quart. Appl. Math. **24**, 107–118 (1966)
11. Willis, J.: Bounds and self-consistent estimates for the overall properties of anisotropic composites. J. Mech. Phys. Solids **25**, 185–202 (1977)
12. Hill, R.: A self-consistent mechanics of composite materials. J. Mech. Phys. Solids **13**, 213–222 (1965)
13. Roscoe, R.: Isotropic composites with elastic or viscoelastic phases: general bounds for the moduli and solutions for special geometries. Rheol. Acta **12**, 404–411 (1973)
14. Mori, T., Tanaka, K.: Average stress in matrix and average elastic energy of materials with misfitting inclusions. Acta Metall. **21**, 571–574 (1973)
15. Benveniste, Y.: A new approach to the application of Mori–Tanaka's theory in composite materials. Mech. Mater. **6**, 147–157 (1987)
16. Christensen, R., Lo, K.: Solutions for effective shear properties in three phase sphere and cylinder models. J. Mech. Phys. Solids **27**, 315–330 (1979)
17. Sheng, P.: Effective-medium theory of sedimentary rocks. Phys. Rev. B **41**, 4507–4512 (1990)
18. Sheng, P., Callegari, A.: Differential effective medium theory of sedimentary rocks. Appl. Phys. Lett. **44**, 738–740 (1984)
19. Nguyen, N., Giraud, A., Grgic, D.: A composite sphere assemblage model for porous oolitic rocks. Int. J. Rock Mech. Min. Sci. **48**, 909–921 (2011)
20. Li, G., Zhao, Y., Pang, S.S.: Four-phase sphere modeling of effective bulk modulus of concrete. Cem. Concr. Res. **29**, 839–845 (1999)
21. Wang, H., Li, Q.: Prediction of elastic modulus and Poisson's ratio for unsaturated concrete. Int. J. Solids Struct. **44**, 1370–1379 (2007)
22. Yaman, I., Aktan, H., Hearn, N.: Active and non-active porosity in concrete part II: evaluation of existing models. Mater. Struct. **35**, 110–116 (2002)
23. Zhu, H.H., Chen, Q., Yan, Z.G., Ju, J.W., Zhou, S.: Micromechanical models for saturated concrete repaired by electrochemical deposition method. Mater. Struct. **47**, 1067–1082 (2014)
24. Yan, Z.G., Chen, Q., Zhu, H.H., Ju, J.W., Zhou, S., Jiang, Z.W.: A multiphase micromechanical model for unsaturated concrete repaired by electrochemical deposition method. Int. J. Solids Struct. **50**, 3875–3885 (2013)
25. Yang, Q.S., Tao, X., Yang, H.: A stepping scheme for predicting effective properties of the multi-inclusion composites. Int. J. Eng. Sci. **45**, 997–1006 (2007)
26. Garboczi, E., Berryman, J.: Elastic moduli of a material containing composite inclusions: Effective medium theory and finite element computations. Mech. Mater. **33**, 455–470 (2001)
27. Chen, H.S., Acrivos, A.: The effective elastic moduli of composite materials containing spherical inclusions at non-dilute concentrations. Int. J. Solids Struct. **14**, 349–364 (1978)
28. Ju, J., Chen, T.M.: Micromechanics and effective moduli of elastic composites containing randomly dispersed ellipsoidal inhomogeneities. Acta Mech. **103**, 103–121 (1994)
29. Ju, J., Chen, T.: Effective elastic moduli of two-phase composites containing randomly dispersed spherical inhomogeneities. Acta Mech. **103**, 123–144 (1994)
30. Ju, J., Sun, L.: A novel formulation for the exterior-point Eshelby's tensor of an ellipsoidal inclusion. J. Appl. Mech. **66**, 570–574 (1999)
31. Ju, J., Zhang, X.: Micromechanics and effective transverse elastic moduli of composites with randomly located aligned circular fibers. Int. J. Solids Struct. **35**, 941–960 (1998)
32. Ju, J., Sun, L.: Effective elastoplastic behavior of metal matrix composites containing randomly located aligned spheroidal inhomogeneities. Part I: micromechanics-based formulation. Int. J. Solids Struct. **38**, 183–201 (2001)
33. Sun, L., Ju, J.: Effective elastoplastic behavior of metal matrix composites containing randomly located aligned spheroidal inhomogeneities. Part II: applications. Int. J. Solids Struct. **38**, 203–225 (2001)

34. Sun, L., Ju, J.: Elastoplastic modeling of metal matrix composites containing randomly located and oriented spheroidal particles. J. Appl. Mech. **71**, 774–785 (2004)
35. Ju, J., Yanase, K.: Micromechanics and effective elastic moduli of particle-reinforced composites with near-field particle interactions. Acta Mech. **215**, 135–153 (2010)
36. Ju, J., Yanase, K.: Micromechanical effective elastic moduli of continuous fiber-reinforced composites with near-field fiber interactions. Acta Mech. **216**, 87–103 (2011)
37. Ju, J., Yanase, K.: Size-dependent probabilistic micromechanical damage mechanics for particle-reinforced metal matrix composites. Int. J. Damage Mech. **20**, 1021–1048 (2011)
38. Yanase, K., Ju, J.W.: Effective elastic moduli of spherical particle reinforced composites containing imperfect interfaces. Int. J. Damage Mech. **21**, 97–127 (2012)
39. Ferrante, F., Graham-Brady, L.: Stochastic simulation of non-Gaussian/non-stationary properties in a functionally graded plate. Comput. Methods Appl. Mech. Eng. **194**, 1675–1692 (2005)
40. Banchs, R.E., Klie, H., Rodriguez, A., Thomas, S.G., Wheeler, M.F.: A neural stochastic multiscale optimization framework for sensor-based parameter estimation. Integr. Comput. Aided Eng. **14**, 213–223 (2007)
41. Biswal, B., Øren, P.-E., Held, R., Bakke, S., Hilfer, R.: Stochastic multiscale model for carbonate rocks. Phys. Rev. E **75**, 1–5 (2007)
42. Chakraborty, A., Rahman, S.: Stochastic multiscale models for fracture analysis of functionally graded materials. Eng. Fract. Mech. **75**, 2062–2086 (2008)
43. Chakraborty, A., Rahman, S.: A parametric study on probabilistic fracture of functionally graded composites by a concurrent multiscale method. Probab. Eng. Mech. **24**, 438–451 (2009)
44. Ganapathysubramanian, B., Zabaras, N.: A stochastic multiscale framework for modeling flow through random heterogeneous porous media. J. Comput. Phys. **228**, 591–618 (2009)
45. Liu, W.K., Siad, L., Tian, R., Lee, S., Lee, D., Yin, X. Lindgen L.E.: Complexity science of multiscale materials via stochastic computations. Int. J. Numer. Methods Eng. **80**, 932–978 (2009)
46. Rahman, S.: Multi-scale fracture of random heterogeneous materials. Ships Offshore Struct. **4**, 261–274 (2009)
47. Yin, X.L., Lee, S., Chen, W., Liu, W.K., Horstemeyer, M.F.: Efficient random field uncertainty propagation in design using multiscale analysis. J. Mech. Des. **131**, 1–10 (2009)
48. Ferrante, F.J., Brady, L.L.G., Acton, K., Arwade, S.R.: An overview of micromechanics based techniques for the analysis of microstructural randomness in functionally graded materials. AIP Conf. Proc. **973**, 190–195 (2008)
49. Rahman, S., Chakraborty, A.: A stochastic micromechanical model for elastic properties of functionally graded materials. Mech. Mater. **39**, 548–563 (2007)
50. Xu, X., Graham-Brady, L.: A stochastic computational method for evaluation of global and local behavior of random elastic media. Comput. Methods Appl. Mech. Eng. **194**, 4362–4385 (2005)
51. Xu, X., Chen, X.: Stochastic homogenization of random elastic multi-phase composites and size quantification of representative volume element. Mech. Mater. **41**, 174–186 (2009)
52. Chen, Q., Zhu, H.H., Ju, J.W., Guo, F., Wang, L.B., Yan, Z.G., Deng, T., Zhou, S.: A stochastic micromechanical model for multiphase composite containing spherical inhomogeneities. Acta Mech. doi:10.1007/s00707-014-1278-y
53. Li, X.J., Chen, X.Q., Zhu, H.H.: Reliability analysis of shield lining sections using Spreadsheet method. Chin. J. Geotech. Eng. **9**, 1642–1649 (2013)
54. Jaynes, E.T.: Information theory and statistical mechanics. Phys. Rev. **106**, 620–630 (1957)
55. Zhu, H.H., Zuo, Y.L., Li, X.J., Deng, J., Zhuang, X.Y.: Estimation of the fracture diameter distributions using the maximum entropy principle. Int. J. Rock Mech. Min. Sci. **72**, 127–137 (2014)
56. Li, X.J., Zuo, Y.L., Zhuang, X.Y., Zhu, H.H.: Estimation of fracture trace length distributions using probability weighted moments and L-moments. Eng. Geol. **168**, 69–85 (2014)
57. Qu, J., Cherkaoui, M.: Fundamentals of Micromechanics of Solids. Wiley, New York (2006)
58. Mura, T.: Micromechanics of Defects in Solids. Kluwer, Dordrecht (1987)
59. Er, G.K.: A method for multi-parameter PDF estimation of random variables. Struct. Saf. **20**, 25–36 (1998)
60. Smith, J.C.: Experimental values for the elastic constants of a particulate-filled glassy polymer. J. Res. NBS **80**, 45–49 (1976)
61. Walsh, J.B., Brace, W.E., England, A.W.: Effect of porosity on compressibility of glass. J. Am. Ceram. Soc. **48**, 605–608 (1965)
62. Weng, G.: Some elastic properties of reinforced solids, with special reference to isotropic ones containing spherical inclusions. Int. J. Eng. Sci. **22**, 845–856 (1984)
63. Weng, G.: The theoretical connection between Mori–Tanaka's theory and the Hashin–Shtrikman–Walpole bounds. Int. J. Eng. Sci. **28**, 1111–1120 (1990)
64. Parameswaran, V., Shukla, A.: Processing and characterization of a model functionally gradient material. J. Mater. Sci. **35**, 21–29 (2000)